Published in final edited form as:

SLAS Technol. 2019 August ; 24(4): 420–428. doi:10.1177/2472630319854337.

Automating a Magnetic 3D Spheroid Model Technology for High-Throughput Screening

Pierre Baillargeon[1], **Justin Shumate**[1], **Shurong Hou**[1], **Virneliz Fernandez-Vega**[1], **Nicholas Marques**[1], **Glauco Souza**[2], **Jan Seldin**[2], **Timothy P. Spicer**[1,†], **Louis Scampavia**[1,*]

[1]The Scripps Research Molecular Screening Center, Department of Molecular Medicine, Scripps Florida, 130 Scripps Way, Jupiter, Florida, USA

[2]Greiner Bio-One, Monroe, NC 28110, USA

Abstract

Affordable and physiologically relevant three-dimensional cell-based assays used in high-throughput screening are on the rise in early drug discovery. These technologies have been aided by the recent adaptation of novel microplate treatments and spheroid culturing techniques. One such technology involves the use of nanoparticle (NanoShuttle-PL) labeled cells and custom magnetic drives to assist in cell aggregation to ensure rapid 3D structure formation after the cells have been dispensed into microtiter plates. Transitioning this technology from a low-throughput manual benchtop application, as previously published by our lab, into a robotically enabled format achieves orders of magnitude greater throughput but required the development of specialized support hardware. This effort included in-house development, fabrication, and testing of ancillary devices that assist robotic handing and high precision placement of microtiter plates into an incubator embedded with magnetic drives. Utilizing a “rapid prototyping” approach facilitated by cloud-based CAD software, we built the necessary components using hobby-grade 3D printers with turnaround times that rival traditional manufacturing/development practices at a substantially reduced cost. This approach culminated in a first-in-class HTS compatible 3D system in which we have coupled 3D bioprinting to a fully automated HTS robotic platform utilizing our novel magnetic incubator shelf assemblies.

Keywords

Spheroid; Organoid; HTS; Magnetic Bioprinting; 3D Printing

[*]Address correspondence to: Louis Scampavia or Timothy P. Spicer, Scripps Florida, 130 Scripps Way #1A1, Jupiter, FL 33458, scampl@scripps.edu, spicert@scripps.edu, 561-228-2101, 561-228-2150.

Shurong Hou is currently located at the Holistic Integrative Pharmacy Institutes, Hangzhou Normal University, Hangzhou, Zhejiang, China

[†]Co-communicated by Timothy P. Spicer

Declaration of Conflicting Interests

The authors declared no potential conflicts of interest with respect to the research, authorship, and/or publication of this article.

Introduction

Efforts to develop HTS methodologies using cultured cells as 3D spheroids and organoids have gained momentum for drug discovery because they are more physiologically relevant than traditional monolayer assays and recently have become more cost effective and less complex for large-scale screening campaigns.[1–4] Technologies that enable cell culture in 3D are referred to as 3D bioprinting and include photolithography, magnetic bioprinting, stereolithography, and direct cell extrusion.[5–10] The most critical, unmet challenge of 3D bioprinting has been scaling production in order to meet the needs of traditional HTS which require hundreds of thousands of wells to be tested for a given campaign.[11] Of the 3D methods currently available, magnetic bioprinting using cell-repellent surface treatment plates from Greiner Bio-One and ultra-low attachment (ULA) microcavity plates from Corning Inc. have proven most promising in their utility to meet the scalability needs of HTS.[12–20]

3D magnetic bioprinting has important advantages for HTS, but also presents hurdles in its integration. The largest challenge is ensuring that magnetic drives are fabricated and installed with sufficient precision for proper alignment of the microtiter plate wells with the magnets found on the drives; all the while remaining as minimally invasive to the system hardware and software components as possible. Enabling this procedure in an HTS environment requires fabricating and installing multiple embedded magnetic drives into the plate incubator; all with acceptable tolerances to minimize drive-to-plate placement variability. Error in this capacity has greater significance for the 1536-well format, where ~2mm wells must align with smaller diameter magnets requiring critical co-alignment in the X and Y-axis within ~100 microns precision. A lack of precision or reproducible accuracy in magnetic drive fabrication can lead to installation and plate handling that is sub-optimal for spheroid development. This constraint is particularly true for applications that may require imaging of the 3D spheroids which is the case in high-content assay approaches.

In this manuscript we are focused on the validation and testing of the Greiner Bio-One m3D and cell-repellent microplate technology to enable 3D bioprinting for HTS, thereby extending previously published techniques for 384-well and 1536-well offline, non-robotic formats to a 1536-well robotic format.[21–23] NanoShuttle-PL employs a nanoparticle assembly technique consisting of gold, iron oxide, and poly-L-lysine. The poly-L-lysine feature facilitates non-specific binding to cell membranes via electrostatic interactions. Once treated with NanoShuttle-PL for a limited period of time, the cells can be aggregated into spheroids or organoids by dispensing the labeled cells into cell-repellent microtiter plates and incubating the plates on top of magnetic drives for a short period of time. Figures 1A and 1B demonstrate how these magnetic drives have been previously used in an offline, non-robotic format. The magnetic drives are designed such that each well of the microtiter plate has a corresponding magnet on the drive which sits under the center of the well and serves as a focal point for cells to aggregate, as seen in the top down view of Figure 1C. Many protocols which make use of this bioprinting technique are primarily focused on 96 and 384 microtiter plate densities, thereby limiting its utility for HTS. Our intention was to make this technique amenable to multi-batch, 1536-well plate format screening and to execute a large-

scale screening initiative to prove that the technique was viable for full robotic automation using a traditional HTS robotic platform.

Additional details regarding the assay biology, usage and validation of m3D technology as compared against a traditional 2D monolayer variant of the assay in an offline, non-robotic capacity can be found in a previously published manuscript from our lab.[23] Herein, we describe the validation and testing of the m3D and cell-repellent microplate technology in 1536-well format to enable 3D bioprinting and prove its utility for fully automated large-scale spheroid and organoid production to support HTS campaigns.

Materials and Methods

Custom Fabrication with CAD

Rapid prototyping of needed hardware was readily facilitated through 3D printing of custom thermoplastic parts; greatly mitigating problems and reducing lengthy turn-around times that traditional methods in engineering experience with fabrication, testing, and redesign.[24, 25] To facilitate the rapid prototyping and testing of custom incubator shelves, we fabricated various magnetic shelf designs using fused deposition modeling 3D printers with polylactic acid (PLA) thermoplastic. A RepRapPro Tricolor Mendel was used to fabricate parts for 384- and 1536-well first-generation prototypes (Figures 1E and 1F) and 384-well second-generation prototypes (Figures 2B and 2D).[26] A SeeMeCNC Rostock Max v2 was used for fabrication of third-generation prototypes (Figure 3A).[27] All in-house produced prototype parts were 3D printed at a layer height of 0.3mm with 100% infill. We designed the custom magnetic shelf CAD models using Onshape[28] and then fabricated them in-house, which allowed many design variants to be tested in a short period of time.

Modification of Shelves

Over the course of this effort, we developed three designs in a sequential fashion with each attempting to address limitations of the previous design. The first- and third-generation designs involved the repurposing of existing magnetic drive assemblies manufactured by n3D Biosciences which were initially provided for non-robotic assay use, while the second-generation design required individual magnetic cylinders to be purchased and inserted directly into the prototype shelf. 3D cell culture system components utilized include flat bottom cell-repellent black wall clear bottom 384-well and 1536-well plates (specialized version of part no. 781976, and 789979, respectively, Greiner Bio-One), 384 and 1536 m3D magnetic spheroid drives (specialized versions of part no. 781835 and 789830, respectively, Greiner Bio-One), and NanoShuttle-PL (part no. 657846, Greiner Bio-One). Note that Greiner Bio-One m3D spheroid drives have also previously been referred to as n3D Bioscience drives prior to acquisition of the technology by Greiner.

HTS System Overview

The facility at Scripps Florida uses a GNF Systems High Throughput Screening (HTS) platform to execute hundreds of biochemical and cell-based assays in either 384- or 1536-well plate format.[29] This platform consists of three integrated, environmentally controllable microtiter plate incubators, two dispensers, a pin tool transfer station, a centrifuge, and a

suite of plate readers. Each of the robotically accessible incubators contain a rotating carousel composed of 18 segmented plate hotel stacks around the incubator's circumference; with each hotel containing 27 shelves for plate placement. Any hotel stack can be readily removed from the carousel. The hotel stacks can be further disassembled to gain access to the individual shelf positions where the microtiter plates reside during incubation. By removing and fully disassembling a shelving unit, seen in Figure 1D, custom magnetic drive shelves can be adapted and installed to create a modified hotel shelf as seen in Figure 3A and its final installation onto the carousel in Figure 4.

Performing Screening Assay

The assay we used to test the function of the first-generation, second-generation and third-generation magnetic drivers was initially developed in 384-well format and then miniaturized to 1536-well format. The protocol that we used for the assay required incubating the assay plates on the magnetic drivers in the following steps: 1) Add NanoShuttle-PL to cells in flask (0.6mL per T175), incubate cells overnight at 37°C, 5% C02, 95% RH, 2) Harvest cells, seed 1250 cells in 5uL culture medium to 1536 Greiner cell repellent plate, 3) Put the plate atop of the spheroid drive, incubate the plate on the drive for 4 hours, 4) Incubate cells for 24 hours at 37 degrees C, 5% CO2, 95% RH, 5) Pintool transfer 10nL compounds, 6) Incubate cells for additional 3 days at 37°C, 5% CO2, 95% RH, 7) Image spheroids using HCS, 8) Dispense 5uL CellTiter-Glo 3D reagent, shake for 10 minutes, incubate 60 minutes at room temperature, read on ViewLux. This assay is described in greater detail in a previous manuscript from our lab which discusses the initial efforts develop this assay and the results of preliminary offline screening in 1536-well format against an internally curated approved drug library of ~3,300 compounds.[23] Concentration response curves (CRC) and IC50 values of pharmacological control compounds were used as a guide for assay optimization and validation for drug screening.

Results and Discussion

First-Generation Design

Our initial design efforts to enable automation of the m3D technology involved adapting the existing lab-bench 384-well magnetic drives onto a custom 3D printed HTS incubator shelf. To make the magnetic drives robotically compatible, we removed the side alignment tabs needed for plate alignment when used with non-robotic assays and seen in Figure 1A. Subsequently, we drilled and tapped alignment holes to allow the drive to be fixed onto the 3D printed HTS incubator shelves.

The first-generation HTS incubator shelf design for the 384-well m3D magnetic drive is seen with and without the magnetic drive installed in Figures 1F and 1E. This design is similar to the stock GNF incubator shelf, Figure 1D, with the exception that the plate platform has been lowered to keep the bottom of each microtiter plate at an equivalent Z-height to a non-modified shelf once the m3D drive has been installed. This design also allows the m3D drive to be fixed into place with three positioning screws in order to ensure accurate alignment needed for proper robotic handling of the microtiter plates onto the shelf. The downside of this approach was that the additional height added to the shelf resulted in

reduced head room of the adjacent shelf below preventing its usage; hence only half of the shelves in any given hotel stack were found to be usable. This limited the initial installation of the modified m3D drive shelves to every other plate location within any given hotel incubator stack.

Second-Generation Design

After this first-generation design was tested and found to be functional, we addressed the primary limitation of the initial design; alternating empty slots in the plate hotel resulting in a loss of HTS capacity due to the height requirements of the initial shelf design. The second-generation design addressed this limitation by incorporating the magnets directly into the incubator shelves as seen in Figures 2B and 2D. The second-generation design had the added benefit of ensuring proper and repeatable magnet alignment relative to the shelf by eliminating Cartesian X and Y axis alignment errors that were possible in the first-generation prototype due to inherent limitations of aligning the magnetic drive and the modified incubator shelf components together. We did not observe these errors during testing, however this is due to significant effort made to ensure proper alignment.

The second-generation 384-well drive used stock magnets that were 1/16” × ¼” cylindrical neodymium magnets from Apex Magnets at a cost of $8.99 per 50 magnets, not including shipping cost.[30] For the 1536-well drive, custom manufactured 3/64” × ¼” cylindrical neodymium magnets were ordered from SM Magnetics at a cost of $1.05 per magnet, not including shipping cost.[31] These custom magnets were ordered with a tolerance of 0.05mm, nickel plated and magnetized through the length of the magnet. Due to the high cost of the magnets for the 1536-well prototype, only 250 magnets were ordered to provide a sufficient quantity to partially populate a 1536-well driver and validate the design.

We found that a limitation of the second-generation design was the need for magnets to be inserted into custom incubator shelving, requiring a mechanical jig to facilitate loading the magnets into the pre-positioned holes without breaking during the press fit. To address this limitation, we designed a magnetic drive jig which sits over the top of the modified shelf during the assembly process to ensure magnets were perpendicular, matched in height, and not damaged during installation. These magnetic installation jigs can be seen to the left of the drives in Figures 2A and 2C for the 384- and 1536-well variant of the second-generation design. Unfortunately, the 1536-well second-generation drive could not be 3D printed using a conventional hobby-grade printer, because the printer lacked the ability to meet acceptable hole-shape tolerances. This problem was resolved by sending the CAD models to Shapeways[32] for professional fabrication using a commercial 3D printer capable of high resolution printing. Parts fabricated by Shapeways were manufactured using Selective Laser Sintering (SLS) with the Shapeways versatile plastic material, also known as nylon plastic or polyamide.[33] We found that the time required to fully assemble a 384-well variant of the second-generation was approximately four hours. For the 1536-well variant of the second-generation design, we partially populated the Shapeways prototype with 250 magnets ordered from SM Magnetics which was sufficient to determine whether or not the design worked in a subset of wells. The amount of time required to insert 250 magnets into the

1536-well second-generation design was also approximately four hours, due to the slightly increased difficulty of handling smaller magnets.

Third-Generation Design

The second-generation drives worked well with robotic testing, however we found the 1536-well magnets to be expensive and the assembly of both the 384- and 1536-well drive shelf to be laborious. A third prototype, seen in Figure 3A, was created which reused preexisting drives obtained from Greiner Bio-One and n3D Biosciences. This design also eliminated the Z-height clearance issue of the first-generation design by installing a set of winged adapters on the sides of the original drive plate. One of the challenges with this third design was ensuring the proper front-to-back alignment of the adapters from drive to drive. To address this constraint, a Y-axis alignment jig, seen in Figure 3B, was designed and 3D printed to enable rapid conversion of the existing drives to work in the HTS incubators. The third-generation jig functions by allowing the user to push the winged adapters against the jig while the jig and face of the magnetic drive were flush, enabling the magnetic drives to be properly aligned at the correct depth in the plate hotel. After aligning the winged adapters, the third-generation jig is removed and the shelf is ready for installation into the incubator.

At each phase of development, the magnetic drive shelves were installed into the robotic incubator (Figure 4) for testing and validation. The magnetic drive shelves can be readily installed or removed from the incubator hotel stack by removing the back plate of the hotel and then installing or removing the drives from any desired location. Each hotel stack can contain upwards of 26 drive plate positions allowing for a nearly full HTS capacity (26 plates per hotel out of 27 possible locations). The bottom location in the hotel stack cannot be modified as it is a structural component of the stack frame. The design of the incubator shelves allows hotel stacks to be quickly swapped, enabling HTS operators to easily replace or alternate between traditional incubator shelves or magnetic drive shelves and providing flexibility to meet the needs of any particular HTS campaign.

One of the primary benefits of the magnetic 3D bioprinting approach is that it requires no significant changes to the HTS platform, nor does it interrupt standard operation apart from the addition of magnetic drives installed within the HTS incubators. Once the drives are installed, the 3D bioprinting assays can commence using established HTS routines with no need of additional support hardware or customized software to complete the adaption.

Screening Assay

To demonstrate the robustness and high-throughput capabilities of 3D spheroid screening, a large-scale screen comprising 151,977 compounds was run using the third-generation m3D magnetic drives (Figure 3A). This screen was performed in a fully automated fashion, testing primary pancreatic cancer cells as 3D organoids under conditions as previously published.[23] The compounds screened were chosen at random from the Scripps Drug Discovery library of 653,085 compounds. To enable this assay to be run on the HTS platform, 10 customized m3D magnetic drives were installed in one of the HTS incubators, which allowed up to two 10 plate batches to be run per day for an average daily throughput of 15,200 compounds per day. At the average daily throughput, the 17 experiments

comprising the pilot screen were completed in 10 days. While throughput for the pilot screen was limited to 20 plates per day in this instance, this limitation was due only to the number of drives currently fabricated. Each HTS incubator has a capacity to hold 468 microtiter plates under the current design and any given hotel stack can be retrofitted to use magnetic drives instead of standard incubator shelves to accommodate the necessary throughput. With a sufficient number of magnetic drives installed, a 3D bioprinting assay could provide the same throughput as a traditional 2D monolayer cell-based assay. A scatterplot of the primary screen plate statistics can be seen in Figure 5A, while a scatterplot of the HTS screen results can be seen in Figures 5B and 5C. Assay plates were determined acceptable only if Z' > 0.5.[34] The response values in the HTS screen results reflect a % inhibition calculation which is defined as 100 * (1 – (Test Well – Median High Control)/(Median Low Control – Median High Control)).[23]

CRC of control compounds in 1536-well offline, non-robotic screening validation results were compared against 1536-well online robotic screening validation results and can be seen in Figures 6A and 6B respectively. As seen in Figures 6C and 6D, previous studies in a traditional 2D monolayer assay also confirmed similar pharmacological responses for hT1 cells with and without the NanoShuttle technology. The specific values calculated from the CRCs can be seen in Table 1. We found the CRC response variances with respect to any given dose remain acceptable and comparable to standard 2D methods; attesting to the reliability of the spheroid production.

For the pilot screen, spheroids were grown from hT1 cells and then quantified using a CellTiter-Glo 3D viability assay. The hT1 cells were derived from patient pancreatic cancer cells intended for use in primary cancer cell research.[35] The pilot screen statistics were monitored with an average Z' factor of 0.72, a signal-to-background ratio of 188.13 and a hit rate of 0.48%. The ability of 3D spheroid formation for hT1 pancreatic cancer cells is different compared to other cells lines like hT29, which is extremely compact with a well-defined surface. 3D formation structures for hT1 cells have been confirmed by Z-stack analysis using confocal microscopy. In addition, the cells were cultured in Corning spheroid plates to test side by side with the 3D bioprinting technology which confirms the spheroid formation is independent of the technology used. This was done to address concerns that the poly-L-lysine (PLL) might interfere with endogenous cell aggregation behavior and resulted in confirmation that the PLL did not interfere as confirmed by previous publications.[12, 21, 36–39] Spheroids produced were found to be uniform as validated previously[23] and by the tight reproducibility of the IC50 values of known anticancer drugs such as doxorubicin. This was assessed using a CRC plate which was included in each robotic HTS run for the 150K initiative which determined doxorubicin to have an average IC50 value of 398nM with only a variance of ~13% (N=17 experiments, 16 replicates per dilution, 3-fold dilutions for ten points).

The 150K screen efforts described in this paper have demonstrated: 1.) 3D bioprinting of spheroids is feasible in a 1536-well format; 2.) Full robotic automation and plate handling can be employed for spheroid production, drug dosing, and plate readout; and 3.) Large-scale HTS screening can be implemented using spheroids in a cost-effective fashion relative to other 3D technologies. When compared to traditional 2D bioassays, bioprinting

techniques using conventional 1536-well microplates were found to be 3-fold higher in cost. However, this compares favorably against bioprinting in specialized microcavity microplates which were found to be 5- to 6-fold higher in cost.

Funding

Research reported in this publication was supported by the National Cancer Institute of the National Institutes of Health under Award Number R33CA206949. The content is solely the responsibility of the authors and does not necessarily represent the official views of the National Institutes of Health.

References

1. Fang Y; Eglen RM Three-Dimensional Cell Cultures in Drug Discovery and Development. SLAS Discovery 2017, 22, 456–472. [PubMed: 28520521]
2. Hirschhaeuser F; Menne H; Dittfeld C; et al. Multicellular tumor spheroids: An underestimated tool is catching up again. Journal of Biotechnology 2010, 148, 3–15. [PubMed: 20097238]
3. Thoma CR; Zimmermann M; Agarkova I; et al. 3D cell culture systems modeling tumor growth determinants in cancer target discovery. Advanced Drug Delivery Reviews 2014, 69–70, 29–41.
4. Longati P; Jia X; Eimer J; et al. 3D pancreatic carcinoma spheroids induce a matrix-rich, chemoresistant phenotype offering a better model for drug testing. BMC Cancer 2013, 13, 95. [PubMed: 23446043]
5. Chua CK; Yeong WY Bioprinting: Principles and Applications. World Scientific Publishing Co. Pte. Ltd.: Singapore, 2014.
6. Ozbolat IT; Moncal KK; Gudapati H Evaluation of bioprinter technologies. Additive Manufacturing 2016.
7. Horman SR; To J; Orth AP An HTS-Compatible 3D Colony Formation Assay to Identify Tumor-Specific Chemotherapeutics. Journal of Biomolecular Screening 2013, 18, 1298–1308. [PubMed: 23918920]
8. Pampaloni F; Reynaud EG; Stelzer EHK The third dimension bridges the gap between cell culture and live tissue. Nature Reviews Molecular Cell Biology 2007, 8, 839–845. [PubMed: 17684528]
9. Banović L; Vihar B Development of an Extruder for Open Source 3D Bioprinting. Journal of Open Hardware 2018, 2, 1.
10. Bajaj P; Chan V; Jeong JH; et al. In 3-D biofabrication using stereolithography for biology and medicine, 2012 Annual International Conference of the IEEE Engineering in Medicine and Biology Society, 28 Aug.−1 Sept. 2012; 2012; pp 6805–6808.
11. Rodríguez-Dévora JI; Zhang B; Reyna D; et al. High throughput miniature drug-screening platform using bioprinting technology. Biofabrication 2012, 4, 035001. [PubMed: 22728820]
12. Tseng H; Gage JA; Shen T; et al. A spheroid toxicity assay using magnetic 3D bioprinting and real-time mobile device-based imaging. Nature Scientific Reports 2015, 5.
13. Fennema E; Rivron N; Rouwkema J; et al. Spheroid culture as a tool for creating 3D complex tissues. Trends in Biotechnology 2013, 31, 108–115. [PubMed: 23336996]
14. Nath S; Devi GR Three-dimensional culture systems in cancer research: Focus on tumor spheroid model. Pharmacology & Therapeutics 2016, 163, 94–108. [PubMed: 27063403]
15. Laschke MW; Menger MD Life is 3D: Boosting Spheroid Function for Tissue Engineering. Trends in Biotechnology 2017, 35, 133–144. [PubMed: 27634310]
16. Lehmann R; Gallert C; Roddelkopf T; et al. Biomek Cell Workstation: A Flexible System for Automated 3D Cell Cultivation. Journal of Laboratory Automation 2016, 21, 568–578. [PubMed: 26203054]
17. Singhera F; Cooper E; Scampavia L; et al. Using bead injection to model dispensing of 3-D multicellular spheroids into microtiter plates. Talanta 2018, 177, 74–76. [PubMed: 29108585]
18. Madoux F; Tanner A; Vessels M; et al. A 1536-Well 3D Viability Assay to Assess the Cytotoxic Effect of Drugs on Spheroids. SLAS Discovery 2017, 22, 516–524. [PubMed: 28346088]

19. Kota S; Hou S; Guerrant W; et al. A novel three-dimensional high-throughput screening approach identifies inducers of a mutant KRAS selective lethal phenotype. Oncogene 2018.
20. Quereda V; Hou S; Madoux F; et al. A Cytotoxic Three-Dimensional-Spheroid, High-Throughput Assay Using Patient-Derived Glioma Stem Cells. SLAS DISCOVERY: Advancing Life Sciences R&D 2018, 23, 842–849. [PubMed: 29750582]
21. Souza GR; Molina JR; Raphael RM; et al. Three-dimensional tissue culture based on magnetic cell levitation. Nature Nanotechnology 2010, 5, 291–296.
22. Baillargeon P; Shumate J; Hou S; et al. Automated, Magnetic Cell Spheroid Formation Within a High-Throughput Screening System. SLAS Technology 2018.
23. Hou S; Tiriac H; Sridharan BP; et al. Advanced Development of Primary Pancreatic Organoid Tumor Models for High-Throughput Phenotypic Drug Screening. SLAS DISCOVERY: Advancing Life Sciences R&D 2018, 23, 574–584. [PubMed: 29673279]
24. Coakley M; Hurt DE 3D Printing in the Laboratory: Maximize Time and Funds with Customized and Open-Source Labware. Journal of Laboratory Automation 2016, 21, 489–495. [PubMed: 27197798]
25. Baden T; Chagas AM; Gage G; et al. Open Labware: 3-D Printing Your Own Lab Equipment. PLOS Biology 2015.
26. RepRapPro Tricolour 3D Printer Page. https://reprap.org/wiki/RepRapPro_Tricolour (accessed November 26, 2018).
27. SeeMeCNC Rostock MAX v2 3D Printer Page. https://makezine.com/product-review/seemecnc-rostock-max-v2/ (accessed November 26, 2018).
28. Onshape Home Page. https://www.onshape.com/ (accessed January 1, 2018).
29. GNF Systems Home Page. http://gnfsystems.com/ (accessed March 8, 2018).
30. Apex Magnets Home Page. http://www.apexmagnets.com (accessed February 28, 2018).
31. SM Magnetics Home Page. http://smmagnetics.com/ (accessed February 28, 2018).
32. Shapeways Home Page. http://www.shapeways.com (accessed February 23, 2018).
33. Shapeways Versatile Plastic Product Description Page. https://www.shapeways.com/materials/versatile-plastic (accessed November 26, 2018).
34. Zhang J-H; Chung TDY; Oldenburg KR A Simple Statistical Parameter for Use in Evaluation and Validation of High Throughput Screening Assays. Journal of Biomolecular Screening 1999, 4, 67–73. [PubMed: 10838414]
35. Boj Sylvia F.; Hwang C-I; Baker Lindsey A.; et al. Organoid Models of Human and Mouse Ductal Pancreatic Cancer. Cell 2015, 160, 324–338. [PubMed: 25557080]
36. Connor EE; Mwamuka J; Gole A; et al. Gold Nanoparticles Are Taken Up by Human Cells but Do Not Cause Acute Cytotoxicity. Small 2005, 1, 325–327. [PubMed: 17193451]
37. Daquinag AC; Souza GR; Kolonin MG Adipose Tissue Engineering in Three-Dimensional Levitation Tissue Culture System Based on Magnetic Nanoparticles. Tissue Engineering Part C: Methods 2013, 19, 336–344. [PubMed: 23017116]
38. Tseng H; Gage JA; Raphael RM; et al. Assembly of a Three-Dimensional Multitype Bronchiole Coculture Model Using Magnetic Levitation. Tissue Engineering Part C: Methods 2013, 19, 665–675. [PubMed: 23301612]
39. Tseng H; Balaoing LR; Grigoryan B; et al. A three-dimensional co-culture model of the aortic valve using magnetic levitation. Acta Biomaterialia 2014, 10, 173–182. [PubMed: 24036238]

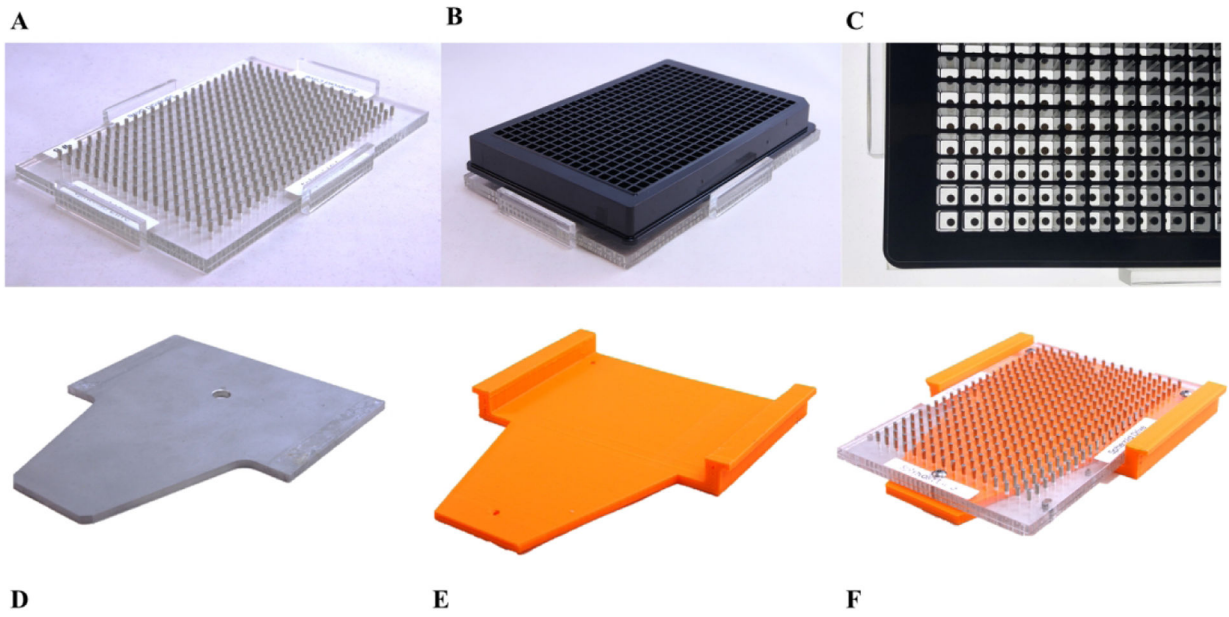

Figure 1.

(**A**) 384-well n3D Bioscience magnetic spheroid drive. (**B**) 384-well n3D Bioscience magnetic spheroid drive with Greiner ULA surface treated microtiter plate (side view). (**C**) 384-well n3D Bioscience magnetic spheroid drive with Greiner ULA surface treated microtiter plate (top view). (**D**) OEM GNF incubator shelf. (**E**) First-generation spheroid drive adapter shelf. (**F**) First-generation spheroid drive adapter shelf with 384-well n3D Bioscience magnetic drive installed.

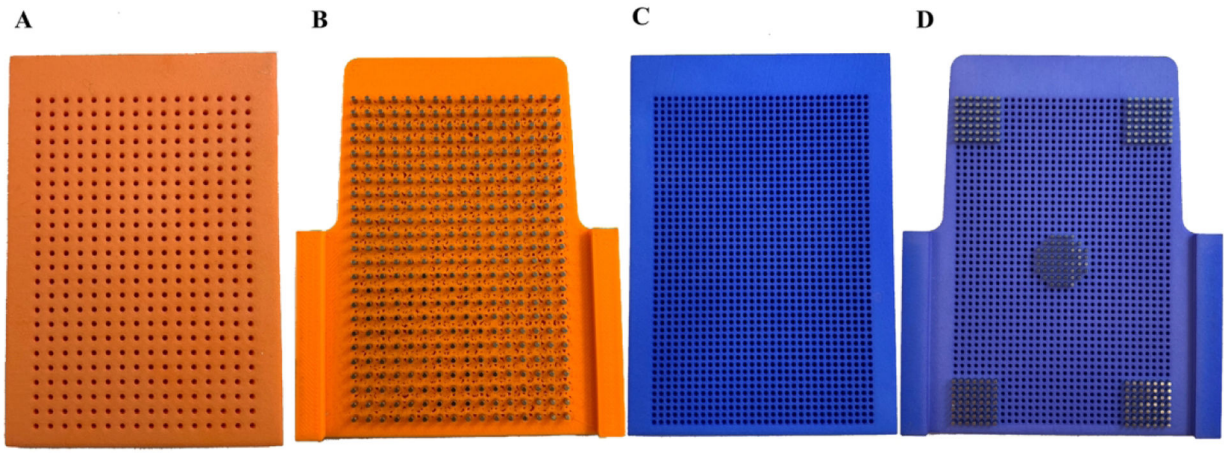

Figure 2.

(**A**) Second-generation HTS incubator 384-well alignment jig. (**B**) Second-generation 384-well spheroid drive. (**C**) Second-generation HTS incubator 1536-well alignment jig. (**D**) Second-generation 1536-well spheroid drive shown partially loaded with magnets.

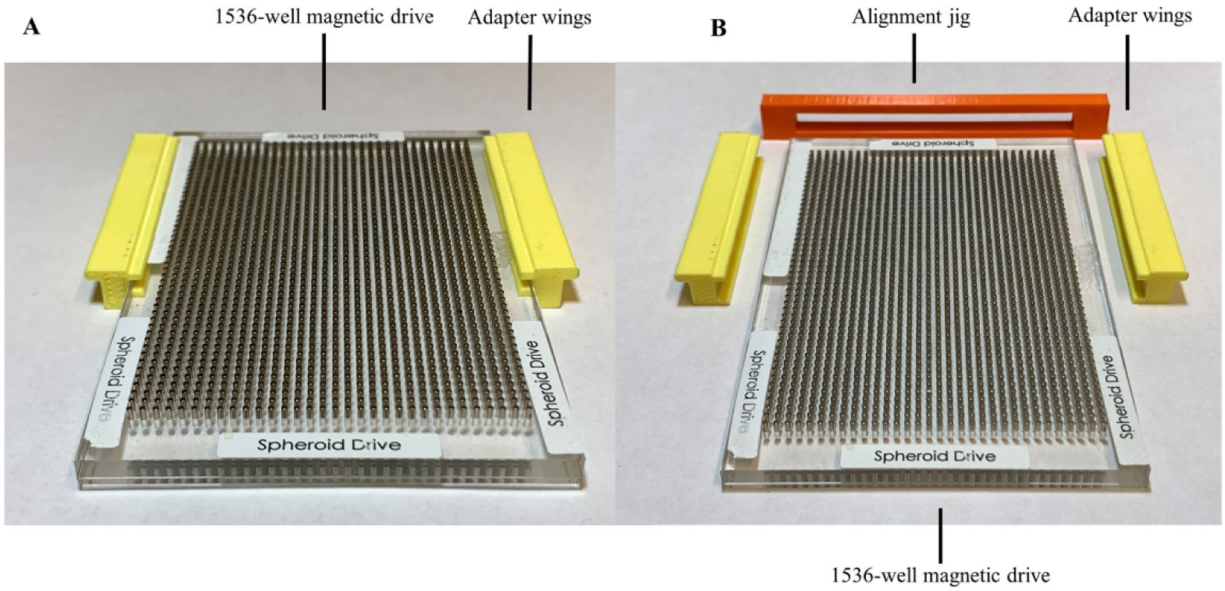

Figure 3.

(**A**) Third-generation n3D Bioscience drive with 3D printed adapter wings installed. (**B**) Third-generation HTS incubator 1536-well spheroid drive with wings uninstalled and alignment bracket for y-axis positioning of wings.

Figure 4.
GNF shelf stack installed into GNF robotic carousel.

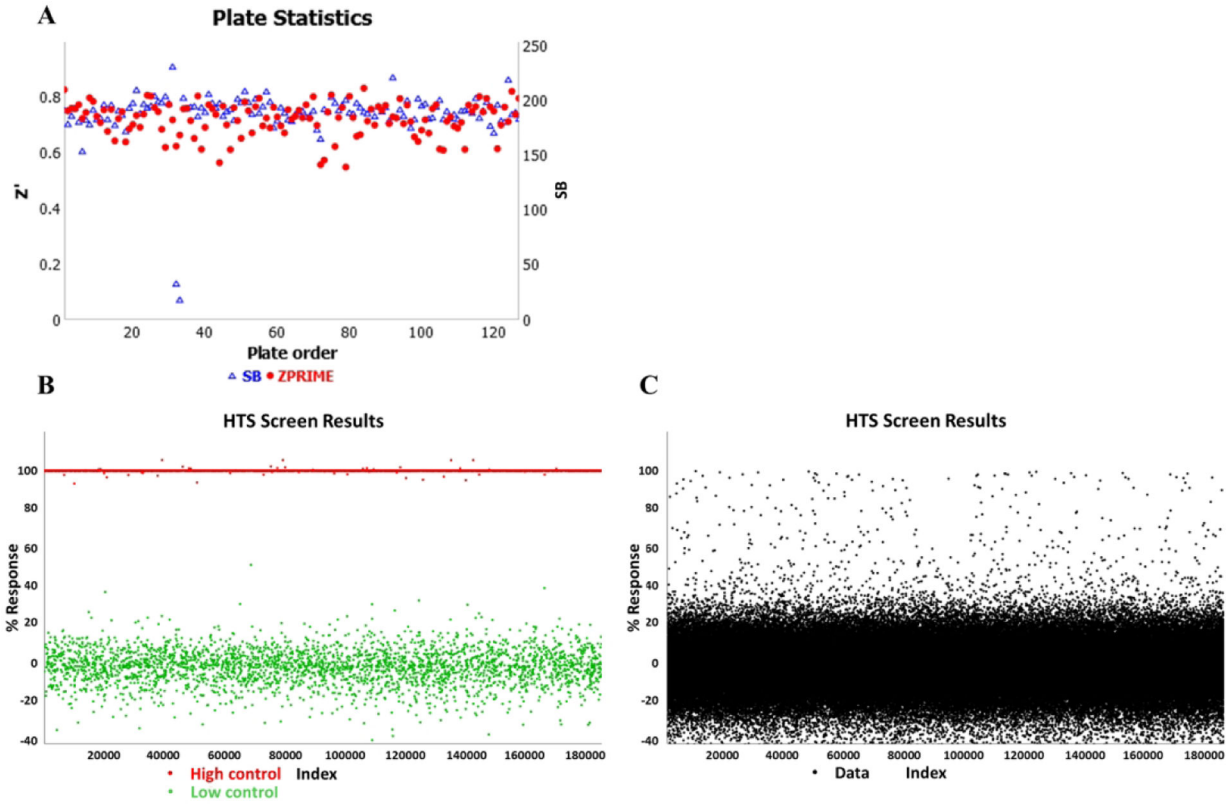

Figure 5.

(**A**) Scatterplot of plate statistics. (**B**) Randomized scatterplot of just the controls form the 150K n3D-KRAS pilot assay. The bottom series of data points near the 0% response point on the chart are low control wells containing cells and DMSO, while the top data points near the 100% response point are high control wells containing medium and DMSO. (**C**) Randomized scatterplot of the 150K n3D-KRAS pilot assay data shown as normalized activity per the controls shown in panel B. Each sample tested is represented by a single black dot.

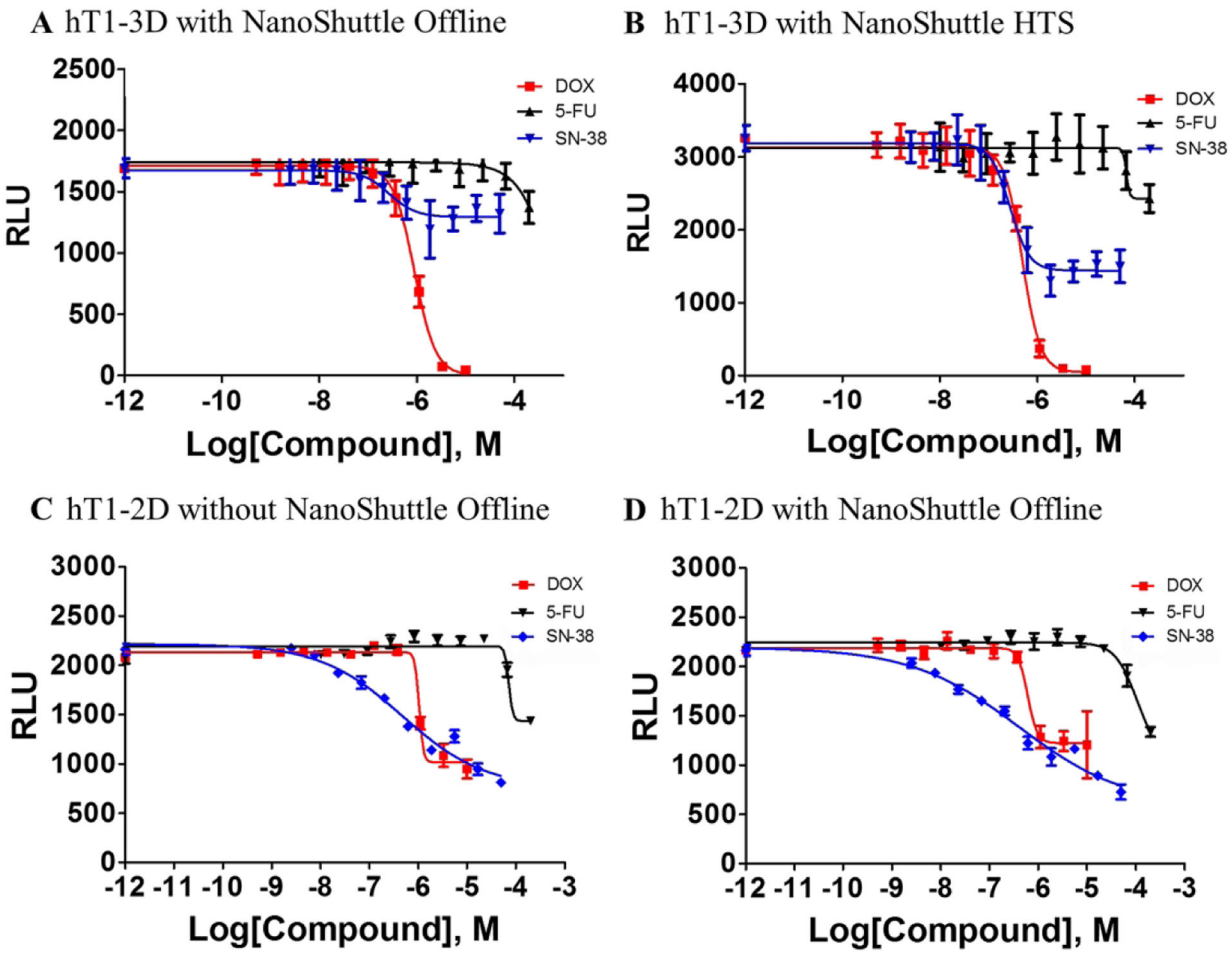

Figure 6.

(**A**) Concentration-response curves for 3 control compounds (doxorubicin, 5-fluorouracil and sn-38) vs. hT1 in 3D formats. CRC results in offline, non-robotic validation run. (**B**) CRC results in online robotic validation run. The curve represents the mean and standard deviation of 16 replicates per each concentration. (**C**) CRC results of hT1–2D cells without NanoShuttle in an offline, non-robotic run. (**D**) CRC results of hT1–2D cells with NanoShuttle in an offline, non-robotic run. All CRC data are shown in Table 1.

Table 1 –

CRC values of control compounds used for robotic validation

	hT1–3D with NanoShuttle Offline			hT1–3D with NanoShuttle Online HTS		
	DOX	**5-FU**	**SN-38**	**DOX**	**5-FU**	**SN-38**
LogIC50	−6.053	−1.059	−6.572	−6.309	~ −4.170	−6.56
HillSlope	−1.995	−1.1	−1.567	−2.353	~ −13.37	−2.188
IC50	8.85E-07	0.08723	2.68E-07	4.91E-07	~ 6.759e-005	2.75E-07
	hT1–2D, without NanoShuttle Offline			**hT1–2D, NON-ROBOTIC with NanoShuttle Offline**		
	DOX	**5-FU**	**SN-38**	**DOX**	**5-FU**	**SN-38**
LogIC50	~ −5.980	~ −4.146	−6.325	−6.216	−3.969	−6.39
HillSlope	~ −10.31	~ −10.87	−0.514	−4.49	−1.907	−0.3918
IC50	~ 1.046e-06	~ 7.141e-05	4.73E-07	6.08E-07	0.0001073	4.07E-07